Preamble

Although the coursework was initially presented as a C++ project, I took the liberty of rewriting the Ising Model system in a programming language called Google Go (https://golang.org). The motivation for this is Go has been designed to accommodate systems with high concurrency. This means that instead of simulating 1 system at a time, 10,000 different systems can be simulated simultaneously in different threads. This greatly increases time efficiency and has allowed me to achieve a significant level of statistical significance in my ensemble averages. Furthermore, this has also allowed me to use ergodicity to calculate time averages for a system ran over a long time period, for many different values of beta at the same time. To achieve the highest possible concurrent number of simulations, the results presented here were generated on a 32-core virtual private server. The source code for my implementation is accessible on Github: `http://tiny.cc/brb75y`.

Comparison of Curie-Weiss Theory and Metropolis Monte Carlo Simulations for Modelling Phase Transitions in Ferromagnets using a Two-Dimensional Ising Model

Candidate Number: 21594
Department of Physics, University of Bath, Bath BA2 7AY, United Kingdom

Abstract. TODO

1. Introduction and Background Theory

Ferromagnetism is the property of a material to exhibit speontaneous magnetisation in the absence of an external magnetic field. The Ising Model is a mathematical model that uses the results of thermodynamics and statistical mechanics to describe how magnetic structure in some metals leads to ferromagnetism [2]. In the Ising Model presented in this paper, a magnetic material is modelled by a regular L x L dimensional square lattice Π. A given grid point on this lattice $\pi_{(i,j)} \in \Pi$ is indexed by cartesian coordinates (i, j) where $i, j \in [0, L]$. These coordinates are not strictly unique as periodic boundary conditions are applied so that a closed system is modelled. This is to say that the grid follows the mappings $(i + \Lambda_i D, j + \Lambda_j D) \to (i, j)$ for $\Lambda_i, \Lambda_j \in \mathbb{Z}$. Each grid point $\pi_{(i,j)}$ on this square lattice is assigned a discrete variable $s_{(i,j)} \in \{0, 1\}$ that corresponds to the spin of the grid point. The system is therefore composed of $N \equiv L^2$ spins. We arbitrarily define $s_{(i,j)} = 1$ to represent 'spin up' and $s_{(i,j)} = -1$ to represent 'spin down'. For a given grid point $\pi_{(i,j)}$, the convention of nearest neighbours is defined as representing the grid points directly adjacent to $\pi_{(i,j)}$, both vertically and horizontally, as shown in Figure 1. Using this convention, the energy of a given spin on the grid is defined as [2]

$$E_{(i,j)} = -h_{(i,j)} s_{(i,j)} \tag{1}$$

where

$$h_{(i,j)} = \sum_{(\alpha,\beta) \text{ n.n. of } (i,j)} \left[J s_{(\alpha,\beta)} \right] \tag{2}$$

Here "n.n" represents a sum over nearest neighbours and J is a positive real number with dimensions of energy that indicates the strength of the interactions between spins. Qualitatively, this set of equations defines the energy of a given spin as the sum of the interaction energies between the spin and it's nearest neighbours, where the interaction energy between two nearest neighbour spins is defined to be $-J$ if the two spins are aligned and $+J$ if the two spins are antiparallel [2], as shown in Figure 2.

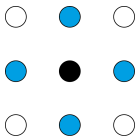

Figure 1: Each dot represents a grid point on the square lattice Π. The central black grid point represents the grid point $\pi_{(i,j)}$. The blue grid points represent the nearest neighbours of $\pi_{(i,j)}$. The white grid points represent points that are not considered nearest neighbours.

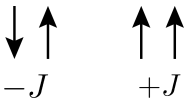

Figure 2: Two nearest neighbour spins on the grid have an interaction energy of $-J$ if they are aligned and $+J$ if they are not aligned.

From this definition of the energy for a single spin in the system, the total energy for the system is defined as

$$E = \frac{1}{2}\sum_{i,j} E_{(i,j)} \tag{3}$$

where the summation simply runs over every grid point in the square lattice. Furthermore, the magnetisation (per spin) of the system is defined as

$$\mathcal{M} = \frac{1}{N}\sum_{i,j} s_{(i,j)} \tag{4}$$

As the number of spins in the system is fixed, a canonical thermodynamic ensemble can be used to model the statistical behaviour of the system. If we let a microstate $\mathcal{S}$ be defined by the instantaneous configuration of all the spins in the system, then the probability of finding the system in a microstate S in thermal equilibrium with a heat bath at temperature T is given by statistical mechanics as [3] [2]

$$p_{eq}(\mathcal{S}) = \frac{1}{Z(T)} e^{-E(S)/k_B T} \tag{5}$$

where $E(S)$ is the energy of microstate S as given by equation (3) and k_B is the Boltzmann constant. The canonical partition function $Z = Z(T)$ is used to enforce the normalisation condition $\sum_S p_{eq}(S) = 1$ which gives the expression for Z as

$$Z(T) = \sum_S e^{-E(S)/k_B T} \tag{6}$$

where the summations here run over all 2^N possible microstates S of the system.

In this paper, a Metropolis Monte Carlo method is used to investigate the properties E and $\mathcal{M}$ of two dimensional Ising Model systems for different thermodynamic temperatures T. In the interest of being concise, for details on how the Metropolis Monte Carlo method works and is implemented, I refer the reader to standard literature [4]. In addition, we compare computational results with those given by a Curie-Weiss (mean-field) theory, the derivation and results of which are described in [2] and, in more detail, the chapter 'Phase Transitions and Critical Phenomena' of [1].

It is important to note that, in the computational simulations used in this paper, the Ising systems are characterised by a dimensionless temperature $T_0 \equiv \frac{Tk_B}{J}$. From this, we define the inverse dimensionless temperature $\beta \equiv \frac{1}{T_0}$.

2. Method

2.1. Calculating Equilibrium Averages

Instead of calculating averages using an ensemble average as is conventional for statistical mechanical systems, it is in most cases also possible to calculate an average $\langle\Gamma\rangle$ for a quantity of interest Γ by taking a time average, where time is proportional to the number of Monte Carlo sweeps completed in our case. This is the ergodic hypothesis of thermodynamics [3]. For the case of a simulated Ising system, this means that average values can be determined by running a single simulation for a period of time as opposed to running many distinct simulations of that one system. In this way, an average value $\langle\Gamma\rangle$ is determined by taking n samples $\{\Gamma_i\}_{i=1}^n$ over a period of time. The average value is then calculated by [2]

$$\langle\Gamma\rangle = \frac{1}{n}\sum_{i=1}^{n} \Gamma_i \tag{7}$$

For independent measurements, the uncertainty in this average is estimated well by standard error.

When calculating equilibrium averages for properties of an Ising system, it is important to ensure the system has reached thermodynamic equilibrium before starting to take samples of the quantity being averaged. For all equilibrium averages presented in this paper, an integer n_0 of Monte Carlo cycles are waited before sampling is begun. This is to give the system time to evolve through its initial transient behaviour as the system changes from the initial all spin down configuration to a state of equilibrium characterised by the thermodynamic temperature of the system. Furthermore, as the Metropolis Monte Carlo algorithm used in this paper is based on a Markovian random walk of phase space, subsequent samples of Γ are very likely to exhibit autocorrelation. Consequently, if a time average $\langle\Gamma\rangle$ is to be representative of the system's entire equilibrium distribution for a practical number of samples n, it is necessary to only sample Γ every $\Delta \in \mathbb{Z}^+$ Monte Carlo sweeps. This increases the likelihood that subsequent samples are independent. So, to account for both initial transient behaviour and to reduce the effect of autocorrelation, samples for equilibrium averages in this paper are taken at Monte Carlo times (sweep numbers)

$$t_i = n_0 + i\Delta \tag{8}$$

2.2. Calculating Derived Quantities

It can be shown that the specific heat capacity c and the magnetic susceptibility χ of an Ising system are determinable by the equations [2]

$$c = \frac{1}{Nk_BT^2}\mathrm{Var}(E) \tag{9}$$

$$\chi = \frac{N}{k_BT}\mathrm{Var}(\mathcal{M}) \tag{10}$$

where T is the thermodynamic temperature of the Ising system and $\mathrm{Var}(E)$ and $\mathrm{Var}(\mathcal{M})$ refer to the variance of the system energy and magnetisation respectively.

3. Results

3.1. Convergence to Equilibrium

An Ising model simulation was prepared with all spins initially down. For different values of system temperature, as defined by the parameter β, the system was computationally simulated using the Metropolis Monte Carlo algorithm. The system's magnetisation per spin $\mathcal{M}$ and dimensionless energy E/J were recorded as the number of Monte Carlo sweeps of the system was increased from 0 to 50. For each value of β, this simulation was run for an ensemble of $10,000$ independent sub-systems, each with different pseudo-random number generator seeds. The evolution of system magnetisation as the number of Monte Carlo sweeps completed increases is shown in Figure 3 (a). Similarly, Figure 3 (b) shows the evolution of the system's dimensionless energy E/J as the number of Monte Carlo sweeps increases.

3.2. Measuring Equilibrium Averages

Figure 4 shows averages of quantities of interest as a function of dimensionless temperature T_0 for an Ising system in thermal equilibrium. Figure 4 (a) shows the average magnetisation per spin as a function of T_0. Figure 4 (b) shows the average dimensionless energy per spin as a function of T_0. Figure 4 (c) shows the average of the absolute value of the magnetisation per spin as a function of T_0. For each of these graphs, the average value of interest is determined for dimensionless temperatures $T_0 \in [1, 4]$ in discrete steps of $\Delta T_0 = 0.005$. Each average is calculated from 990 samples. The times that these samples were taken at is described by equation (8) with values $n_0 = 2000$ and $\Delta = 200$.

3.3. Mean Field Theory

Figure 5 shows the mean field theory results for quantities of interest in the Ising model. Figure 5 (a) shows mean field theory results for the magnetisation per spin. Figure 5 (b) shows results for the dimensionless energy per spin. Figure 5 (c) shows results for the dimensionless heat capacity. Figure 5 (d) shows results for the magnetic susceptibility.

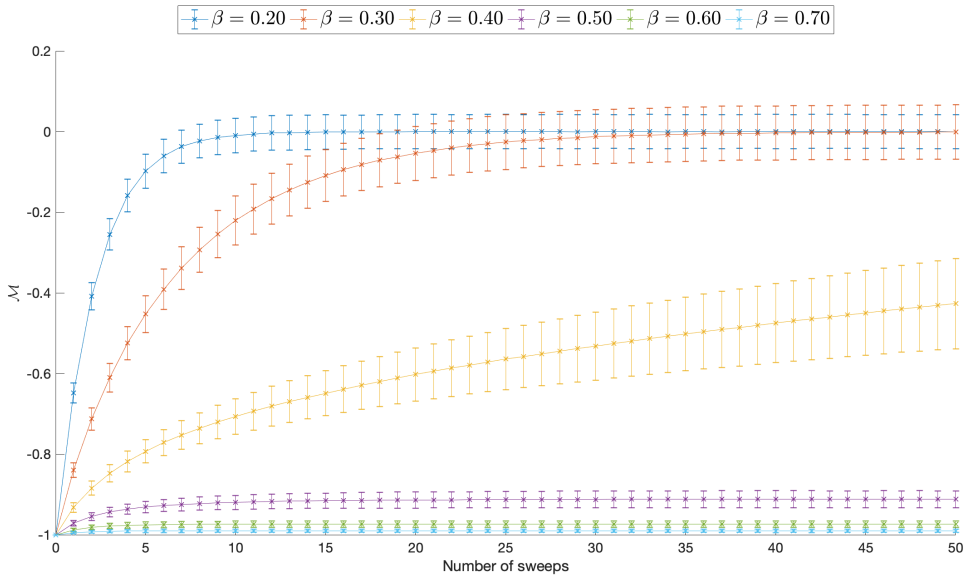

(a) Evolution of system magnetisation per spin

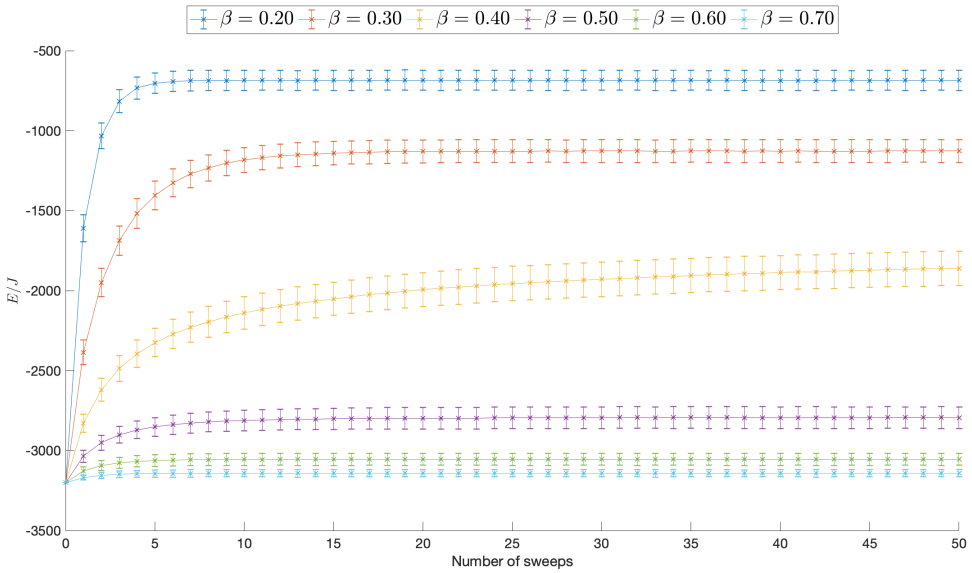

(b) Evolution of total system energy

Figure 3: Evolution of (a) system magnetisation per spin and (b) total system energy as a function of the number of Monte Carlo sweeps completed for a 2D Ising model simulation with all spins initially down. The simulation was ran for a set of systems with different thermodynamic temperatures, as defined by the parameter β. Each data point represents the ensemble average over $10,000$ independent sub-systems, each initialised with different pesudo-random number generator seeds. Error bars represent the standard deviation in the values of (a) $\mathcal{M}$ and (b) $\frac{E}{J}$ across the ensemble of systems.

3.4. Specific Heat Capacitiy and Magnetic Susceptibility

Figure 6 shows quantities derived from the data shown in Figure 4. Figure 6 (a) is a plot of a dimensionless quantity that is proportional to heat capacity as a function of dimensionless system temperature T_0. Figure 6 (b) is a plot of a dimensionless quantity that is proportional to magnetic susceptibility.

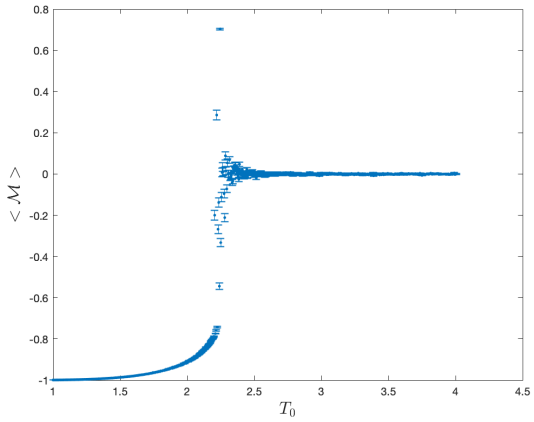

(a) Average magnetisation per spin

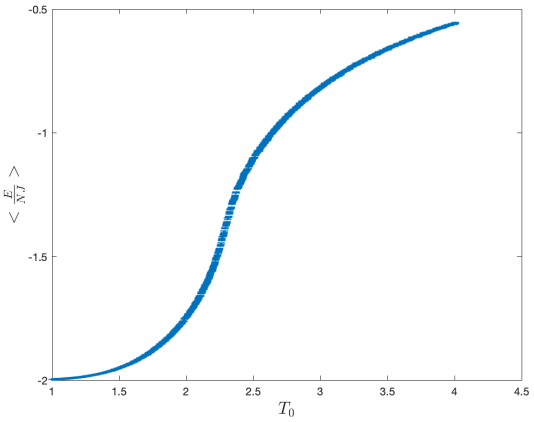

(b) Average dimensionless energy per spin

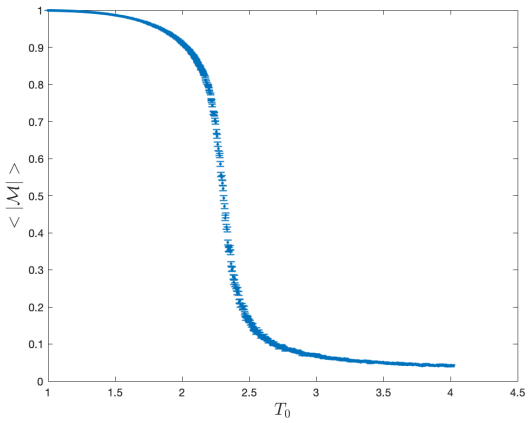

(c) Average absolute magnetisation per spin

Figure 4: Averages of quantities as given by equation (7) of interest as a function of dimensionless temperature T_0 for an Ising system in thermal equilibrium. (a) shows average magnetisation per spin $\langle \mathcal{M} \rangle$ vs T_0. (b) shows average dimensionless energy per spin $\langle \frac{E}{NJ} \rangle$ vs T_0. (c) shows average absolute magnetisation per spin $\langle |\mathcal{M}| \rangle$ vs T_0. Each average is determined from 990 samples given by equation (8) with $n_0 = 2000$ and $\Delta = 200$. Error bars represent standard errors.

4. Discussion

4.1. Convergence to Equilibrium

For cases where the system evolves into a state with $\mathcal{M} = 0$, which is characterised by the system being in a state with approximately half the spins up and half the spins down, Figure 3 (a) shows that an inverse temperature of $\beta = 0.3$ takes longer to converge to this equilibrium state than $\beta = 0.2$.

4.2. Equilibrium Averages

Figure 4 (a) shows an increase in system magnetisation from an initial value of -1 to approximately -0.8 as T_0 is increased from 1 to approximately 2.3. This corresponds to the system transitioning from an initial perfectly ferromagnetic order with all spins down to more energetic states with ferrimagnetic order where some spins are up but the majority are still down, resulting in a net negative magnetisation. The simulated Ising model then almost-perfectly captures a phase transition at a critical dimensionless temperature of $T_{0,c} \approx 2.3$, at which point the system almost instantaneously assumes paramagnetic order for which $\mathcal{M} = 0$ in the absence of an external magnetic field. For all temperatures greater than this critical temperature, no change in magnetisation is exhibited. Note somewhat weird behaviour is exhibited during the phase transition where the magnetisation appears to diverge and becomes

greater than 0. This could be physical or could simply be that the system is so chaotic during this transition that Monte Carlo averaging breaks down and fails to capture the true behaviour of the system. Additionally, although a discontinuity exists in the magnetisation during the phase transition, the system's energy increases continuously during the transition, as physically expected!

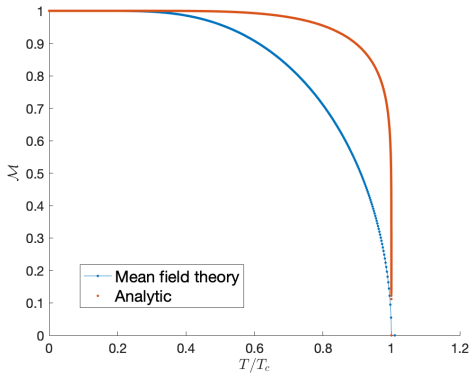

(a) Magnetisation per spin

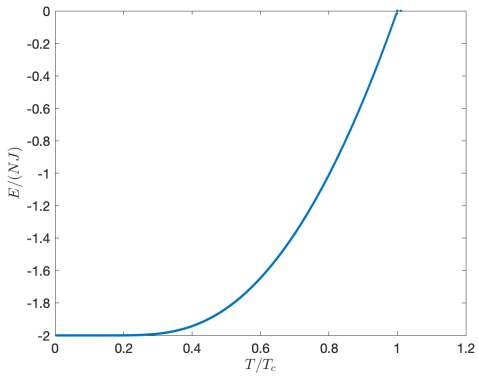

(b) Dimensionless energy per spin

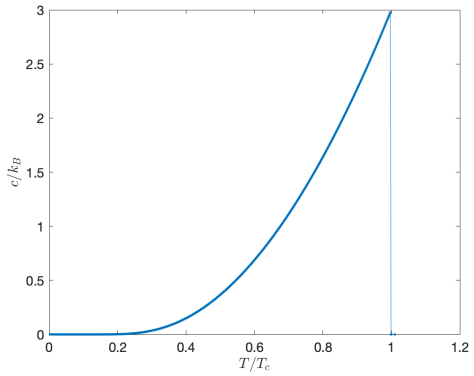

(c) Dimensionless heat capacity

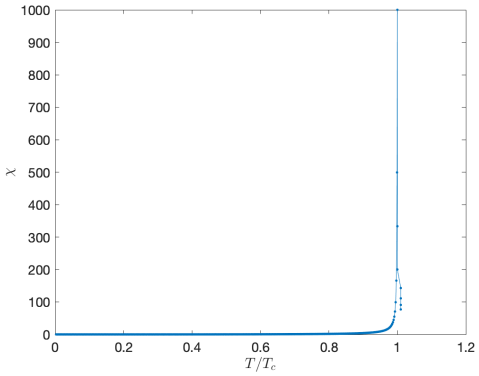

(d) Magnetic Susceptibility

Figure 5: Mean field theory results for (a) the magnetisation per spin, (b) the dimensionless energy per spin, (c) dimensionless heat capacity and (d) magnetic susceptibility as a function of a dimensionless temperature parameter T/T_c. (a) also shows the analytic value of the magnetisation per spin as given in [2].

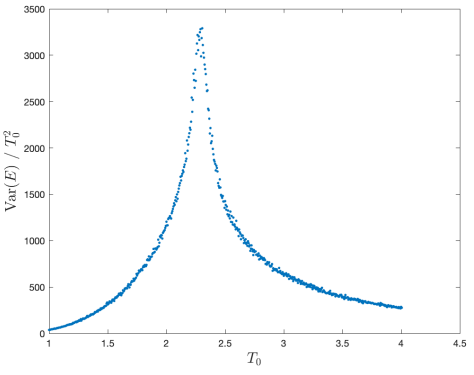

(a) Heat capacity

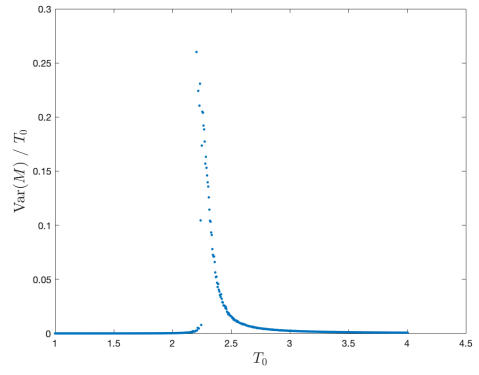

(b) Magnetic susceptibility

Figure 6: Computational Monte Carlo results for dimensionless quantities that are proportional to (a) heat capacity and (b) magnetic susceptibility. Calculated from the data given in Figure 4.

4.3. Evaluation of Mean-Field Theory

Comparison of Figures 4 (c) and 5 (a) shows that mean field theory is in agreement with the Monte Carlo simulations for the behaviour of the system magnetisation $\mathcal{M}$ up to the critical temperature T_c at which the phase transition occurs. In addition, inspection of Figure 5 shows that the mean field approximation to the magnetisation is a good approximation to the analytic energy at both low temperatures and at the phase transition. In between however, mean field theory starts decreasing from 1 to 0 much earlier than the analytic solution. Comparison of Figures 4 (b) and 5 (b) shows that mean field theory gives a very good approximation to the behaviour of the total system energy up until the critical dimensionless temperature at $T_{0,c} \approx 2.3$. Comparison of Figures 5 (c) and 6 (a) shows that mean field theory agrees fairly well with Monte Carlo simulations in the region between $T = 0$ and the phase transition. However, immediately after the phase transition, mean field theory gives a heat capacity of $c \approx 0$ whereas Monte Carlo simulations give a heat capacity distribution that peaks at the phase transition and then decreases after the transition in a manner that is almost symmetric about the critical temperature.

4.4. Derivative Quantities

By inspection, it is immediately apparent that the heat capacity shown in Figure 6 (a) as determined using equation (9) is consistent with the definition of heat capacity as $c = \frac{\partial}{\partial T}\langle E/N \rangle$ [2] as the shape of Figure 6 (a) nicely reflects the gradient of Figure 4 (a).

4.5. Suggestions for Improvement

In this paper, when calculating equilibrium averages, the number of Monte Carlo sweeps that were skipped n_0 was simply made very large so there was a negligible chance of initial transient behaviour affecting the calculated averages. A more efficient approach to this would be to calculate and use the autocorrelation function for each quantity being averaged so that the smallest number of sweeps possible is skipped, as presented in [5].

5. Conclusion

References

[1] Modern Problems of Molecular Physics : Selected Reviews from the 7th International Conference "Physics of Liquid Matter: Modern Problems", Kyiv, Ukraine, May 27–31, 2016. Springer Proceedings in Physics, 197. Springer International Publishing : Imprint: Springer, Cham, 2018.

[2] RLJ AS, VJTR. Ising model coursework handout. ph30056 comp phys b – coursework 2: Ising model. Handout, 05 2019.

[3] R. (Raymond) Jancel. Foundations of classical and quantum statistical mechanics. International series of monographs in natural philosophy ; Volume 19. Pergamon Press, Oxford, [England], first english edition. edition, 1969.

[4] Tao Pang. An Introduction to Quantum Monte Carlo Methods. 2053-2571. Morgan and Claypool Publishers, 2016.

[5] Ohio State University. Notes on the ising model from 6810 computational physics. accessed online on 06/05/2019. `https://www.asc.ohio-state.edu/physics/ntg/6805/readings/ising_model.pdf`.